Numerical solution for the flow over a stretchable disk

Sajjad Hussain[1], Dr. Farooq Ahmad[2] , M. Shafique [3]
[1] *sajjad_h96@yahoo.com,* [2]*farooqgujar@gmail.com,* [3]*mshafique6161@hotmail.com*
[1]Centre for Advanced Studies in Pure and Applied Mathematics, B. Z. Uni., Multan, Pakistan
[2] Punjab Higher Education Department, Principal, Govt. Degree College Darya Khan, (Bhakkar)
[3] Department of Mathematics, Gomal University, D. I. Khan,
PAKISTAN

ABSTRACT

Numerical solution is obtained for the flow over a stretchable disk with or without rotation. Similarity transformations are used to convert the highly non linear governing partial differential equations to their ordinary differential form. The transformed equations have been solved numerically, using SOR method and Simpson's (1/3) rule. The numerical results have been improved by Richardson's extrapolation. The velocity and pressure distributions have been obtained for various values of disk rotation parameter s. When s=0, the flow corresponds to purely stretchable disk and when s>0, the flow is related to a stretching and rotating disk.

AMS Subject Classification: 76M20.

Keywords: Newtonian fluid, Navier-stokes model, stretchable disk, Similarity transformations, Richardson's extrapolation.

I. INTRODUCTION

The fluid flow due to stretchable surface bears important application in extrusion process in plastic and metal industries. Sakiadas [1, 2] examined the boundary layer flow on a continuously stretching surface with a constant speed. Crane [3] obtained a similarity solution in closed analytical form for steady two dimensional incompressible boundary layer flow caused by the stretching of a sheet. Wang [4] studied the fluid flow problem due to stretching boundary for three dimensional case. Chiam [5] investigated steady two dimensional stagnation point flow of an incompressible fluid towards a stretching surface. Mahapatra and Gupta [6, 7] combined both the stagnation point flow and stretching surface. Several researchers including Carragher and Crane [8], Gupta and Gupta [9], Liao and Pop [10] studied different aspects of fluid flow due to moving boundaries. Shafique and Rashid [11] examined the three dimensional fluid motion caused by the stretching of a flat surface. S. Hussain and M. Kamal [12] examined flow of micropolar fluid flow over a stretchable disk.

Ever since Von Karman [13] derived the simplified equations that govern the flow over a rotating disk, this problem and many variations of it have attracted several classical text books e.g.[14,15]and researchers. The boundary layer transition and stability of rotating disk flow has been studied by [16, 17]. S. Hussain et al [18] obtained numerical solution of a decelerated rotating disk in a viscous fluid. Fang [19] obtained exact solution for steady state Navier-Stokes

equations governing the flow over a stretchable disk.

In this paper, the problem of Fang [19] has been studied numerically by using SOR method, Richardson's extrapolation and Simpson's (1/3) rule for rang $0 \le s \le 500$. Fang [19] obtained solution of the problem for range $0 \le s \le 200$. The calculations have been carried out using three different grid sizes to check the accuracy of the results. The present numerical results have also been compared with the previous results and found in good agreement. Our numerical scheme is easy, straightforward and efficient.

II. Mathematical Analysis

The flow is steady and incompressible. The cylindrical coordinates (*r,θ, z)* are used, *r* being the radial distance from the axis, θ the polar angle and *z* the normal distance from the disk. The body force and the body couple are neglected [12]. The Navier-Stokes equations in components form are given below

$$u_r + \frac{u}{r} + \frac{1}{r} v_\theta + w_z = 0 \tag{1}$$

$$uu_r + \frac{v}{r} u_\theta + wu_z - \frac{v^2}{r} = -\frac{1}{\rho} p_r + \nu\left(\frac{u}{r^2} + \frac{1}{r^2} u_{\theta\theta} - \frac{2}{r^2} v_\theta + u_{zz}\right) \tag{2}$$

$$uv_r + \frac{v}{r} v_\theta + wv_z + \frac{uv}{r} = -\frac{1}{r\rho} p_\theta + \nu\left(v_{rr} + \frac{1}{r} v_r - \frac{v}{r^2} + \frac{1}{r^2} v_{\theta\theta} + \frac{2}{r^2} u_\theta + v_{zz}\right) \tag{3}$$

$$uw_r + \frac{v}{r} w_\theta + ww_z = -\frac{1}{\rho} p_z + \nu\left(w_{rr} + \frac{1}{r} w_r + \frac{1}{r^2} w_{\theta\theta} + w_{zz}\right) \tag{4}$$

The following similarity transformations are used.

$$u = r\omega F(\eta),\ v = r\omega G(\eta), w = \sqrt{\omega\nu}\, H(\eta),\ p = \rho\nu\omega P(\eta) \tag{5}$$

where $\eta = \sqrt{\frac{\omega}{\nu}} z$ is the similarity variable, ν being kinematics viscosity.

The equations (1) to (4) become:

$$2F + H' = 0 \tag{6}$$

$$F^2 - G^2 + HF' = F'' \tag{7}$$

$$2FG + HG' = G'' \tag{8}$$

$$-HH' - 2F' = P' \tag{9}$$

where primes denote differentiation with respect to η.

The boundary conditions are:

$$\eta = 0:\ F = 0,\ G = s,\ H = 0, P = 0 \qquad \eta \to \infty : F = 0, G = 0 \tag{10}$$

where *s* shows the disk rotation strength relative to the disk stretching strength and named as the disk rotation parameter. It is to be noticed that the similarity equations are obtained when the disk stretching speed is proportional to radius of the disk.

In order to obtain the numerical solution of nonlinear ordinary differential equations (7) and (8), these equations are discritized by central difference approximation at a typical point $\eta = \eta_n$ of the interval [0,∞), we obtain

$$(4 + 2h^2 F_n) F_n = (2 - hH_n) F_{n+1} + (2 + hH_n) F_{n-1} + 2h^2 G^2 n \tag{11}$$

$$(4 + 4h^2 F_n) G_n = (2 - hH_n) G_{n+1} + (2 + hH_n) G_{n-1} \tag{12}$$

ISSN 2350 – 7756

where *h* denotes a grid size and the equation (6) is integrated numerically. Also, the symbols used denote $F_n = F(\eta_n), G_n = G(\eta_n)$ and $H_n = H(\eta_n)$. For computational purposes, we shall replace the interval [0,∞) by [0, b] where b is a sufficiently large.
The pressure equation (9) can be easily integrated to yield

$$P_n = 2. - 0.5(H_n)^2 - 2F_n \qquad (13)$$

with initial condition P(0)=0.

The finite difference equations (11) and (12) are solved by using SOR iterative scheme Hildebrand [20]. The equation (6) is integrated using Simpson's (1/3) rule Gerald [21] along with the formula given in Milne [22]. These equations are solved numerically at each required grid point of interval [0, b] subject to the appropriate boundary conditions.

The SOR procedure gives the solution of *F* and *G* of order of accuracy $O(h^2)$ due to second order finite differences and Simpson's (1/3) rule gives the order of accuracy $O(h^5)$ for the solution of H. Higher order accuracy in the solution of F and *G*, on the basis of above solutions, is achieved by using Richardson's extrapolation to the limit Burden [23].

III. Numerical Results and Discussion

The calculations have been carried out for the values of the parameter *s* in the range $0 \le s \le 500$. In order to check the accuracy of the numerical results for the velocity and pressure distributions, they have been computed on three different grid sizes namely *h*=0.025, *h*=0.0125 and *h*=0.006.The results are in good comparison with the previous results Fang [19].

When the disk rotation parameter *s*=0, the problem corresponds to a flow over a stretchable disk only. In this situation, the flow is caused by the stretching of the disk in the radial direction, hence there is no flow in the circumferential direction and value of *G* remains zero. The numerical solutions for the radial and axial components of velocity *F* and *H* and the pressure *P* are found and presented in table 2.Graphically, the results of these functions are demonstrated in fig.1.The negative direction of the axial velocity component *H* shows that the fluid is drawn towards the wall under the effect of wall stretching. The pressure near the disk is smaller than the pressure in the outer region. In fact, the pressure in the outer region pushes the fluid towards the wall. The numerical result for $F'(0) = -1.736802$ agrees with the result $F'(0) = -1.73721$by Fang [19].

When the rotation parameter *s*>0, the problem corresponds to the flow over a rotating and stretching disk. The results of velocity component *F* and *G* in the higher order accuracy $O(h^6)$ are presented in table 2 for some values of parameter *s*. Tables 4 to 7 show the results calculated by using SOR method and Simpson's (1/3) rule for *F*, *G*, *H* and *P* for finer grid size. Fig.2 shows the radial velocity distribution *F*. The radial velocity component near the disk exceeds the stretching velocity for increasing values of the rotation parameter due to increasing effect of centrifugal force. The behavior of the circumferential velocity *G* is shown in fig.3. The axial velocity *H* increases in the negative z-direction for larger values of the rotation parameter due to the effect of disk rotation as depicted in fig.4.The axial velocity at infinity is shown in fig.7. Also, for increasing values of *s*, the pressure decreases with the increase in magnitude of the axial velocity. The pressure at infinity is shown in fig.8.Figures 5 and 6 depict $-F'(0)$ and $-G'(0)$ for smaller values of *s*. It is noted that the stretching shear force $-F'(0)$ and the rotating shear force

ISSN 2350 – 7756

$-G'(0)$ both increase with for larger values of s as shown in fig.9 and fig.10.The present results for $-H(\infty)$ are compared with the previous results and presented in table 1. The results are in good agreement with the previous results.

Table1: comparison of present and previous results of -$H(\infty)$

s	-$H(\infty)$		s	-$H(\infty)$	
	Present numerical results	Exact results Fang[19]		Present numerical results	Exact results Fang[19]
100	8.8778	8.84	350	16.5733	16.53
150	10.8808	10.82	400	17.7136	17.68
200	12.5439	12.50	450	18.7852	18.75
300	15.3485	15.31	500	19.7964	19.76

Table 2: Numerical results using SOR Method and Simpson's Rule when s=0.0

h	η	F	H	P
0.006	0.000	1.000000	0.000000	0.000000
	1.000	0.268108	-1.134358	0.820400
	2.000	0.062058	-1.417810	0.870791
	3.000	0.013431	-1.481724	0.875384
	4.000	0.002455	-1.494970	0.877621
	5.000	0.000000	-1.496835	0.879743

Table 3: Numerical results using Richardson's Extrapolation Method

	s = 0.5		s = 1.0		s = 5.0		s = 12.0	
η	F	G	F	G	F	G	F	G
0.0	1.000000	0.500000	1.000000	1.000000	1.000000	5.000000	1.000000	12.00000
0.5	0.535498	0.236008	0.560946	0.464197	0.990864	1.779583	1.610962	2.739678
1.0	0.259343	0.107532	0.273048	0.207204	0.410785	0.581111	0.401580	0.547712
1.5	0.112061	0.045372	0.116757	0.085732	0.134882	0.179089	0.081002	0.106055
2.0	0.037291	0.015001	0.038281	0.027862	0.034236	0.044909	0.013599	0.017700
2.5	0.000000	0.000000	0.000000	0.000000	0.000000	0.000000	0.000000	0.000000

Table 4: Numerical results using SOR method and Simpson's rule for finer grid size

s=20					s=25				
η	F	G	H	P	η	F	G	H	P
0.0	1.000000	20.000000	0.000000	0.000000	0.0	1.000000	25.000000	0.000000	0.000000
0.5	1.974522	3.103420	-3.078369	-6.687223	0.5	2.028897	3.082407	-3.593653	-8.514965
1.0	0.297890	0.441044	-3.992418	-6.565481	1.0	0.240142	0.348114	-4.454495	-8.401550
1.5	0.037719	0.064568	-4.118944	-6.558289	1.5	0.024744	0.041718	-4.549553	-8.398707
2.0	0.004295	0.008271	-4.134635	-6.556193	2.0	0.002295	0.004326	-4.559203	-8.397755
2.5	0.000000	0.000000	-4.136082	-6.553586	2.5	0.000000	0.000000	-4.559941	-8.396531

Table 5: Numerical results using SOR method and Simpson's rule for finer grid size

s = 50					s = 100				
η	F	G	H	P	η	F	G	H	P
0.0	1.000000	50.000000	0.000000	0.000000	0.0	1.000000	100.00000	0.000000	0.000000
0.5	1.810169	2.510272	-5.739398	-8.090681	0.5	1.056100	1.399664	-8.657029	-37.584269
1.0	0.081311	0.106121	-6.304691	-18.037185	1.0	0.012418	0.015369	-8.893795	-37.574622
1.5	0.003434	0.004480	-6.329320	-18.037015	1.5	0.000147	0.000191	-8.896570	-37.574765
2.0	0.000139	0.000182	-6.330356	-18.036980	2.0	0.000002	0.000002	-8.896600	-37.574738
2.5	0.000000	0.000000	-6.330393	-18.036939	2.5	0.000000	0.000000	-8.896600	-37.574732

Table 6: Numerical results using SOR method and Simpson's rule for finer grid size

s = 200					s = 300				
η	F	G	H	P	η	F	G	H	P
0.0	1.000000	200.000000	0.000000	0.000000	0.0	1.000000	300.000010	0.000000	0.000000
0.2	13.163144	19.473928	-10.295395	-77.323865	0.2	11.933286	16.713300	-13.721378	-16.004660
0.4	1.207087	1.586798	-12.344481	-76.607286	0.4	0.594834	0.776724	-15.258152	-115.595250
0.6	0.098549	0.128332	-12.521959	-76.596814	0.6	0.027657	0.036001	-15.332169	-115.593000
0.8	0.007420	0.009657	-12.536232	-76.593381	0.8	0.001227	0.001598	-15.335591	-115.592620
1.0	0.000000	0.000000	-12.537153	-76.590079	1.0	0.000000	0.000000	-15.335728	-115.592250

Table 7: Numerical results using SOR method and Simpson's rule for finer grid size

s = 400					s = 500				
η	F	G	H	P	η	F	G	H	P
0.0	1.000000	400.000000	0.000000	0.000000	0.0	1.000000	500.000000	0.000000	0.000000
0.2	10.199916	13.901022	-16.514964	-154.771860	0.2	8.538516	11.460753	-18.894074	-193.570060
0.4	0.308756	0.402487	-17.658889	-154.535710	0.4	0.167849	0.218728	-19.753061	-193.427410
0.6	0.008939	0.011641	-17.692764	-154.534830	0.6	0.003202	0.004173	-19.769698	-193.426900
0.8	0.000251	0.000327	-17.693740	-154.534720	0.8	0.000060	0.000078	-19.770015	-193.426870
1.0	0.000000	0.000000	-17.693763	-154.534630	1.0	0.000000	0.000000	-19.770020	-193.426830

ISSN 2350 – 7756

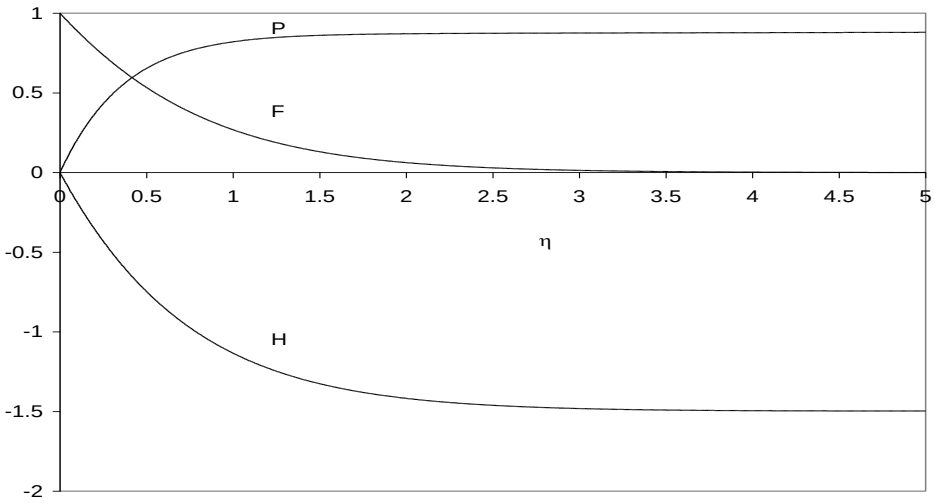

Fig .1: Graph of *F*, *H* and *P* for the case: *s*=0

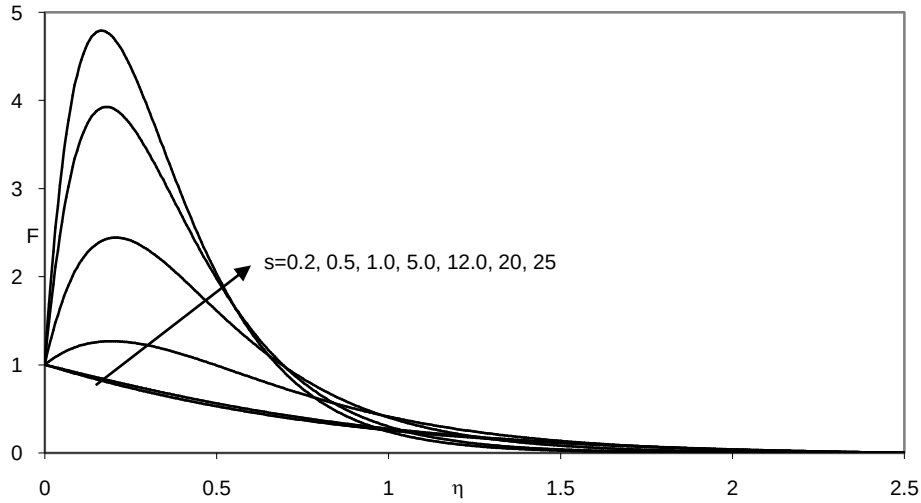

Fig .2: Graph of *F* for different values of the parameter *s*

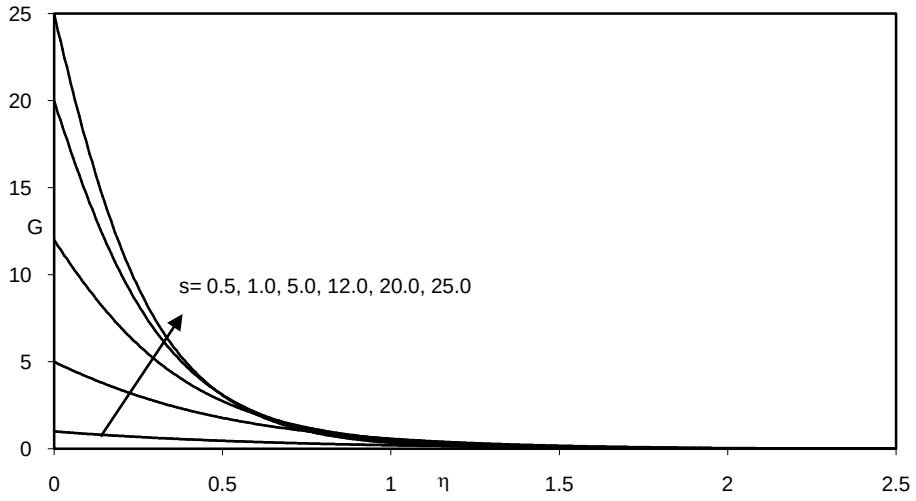

Fig.3: Graph of *G* for different values of the parameter *s*

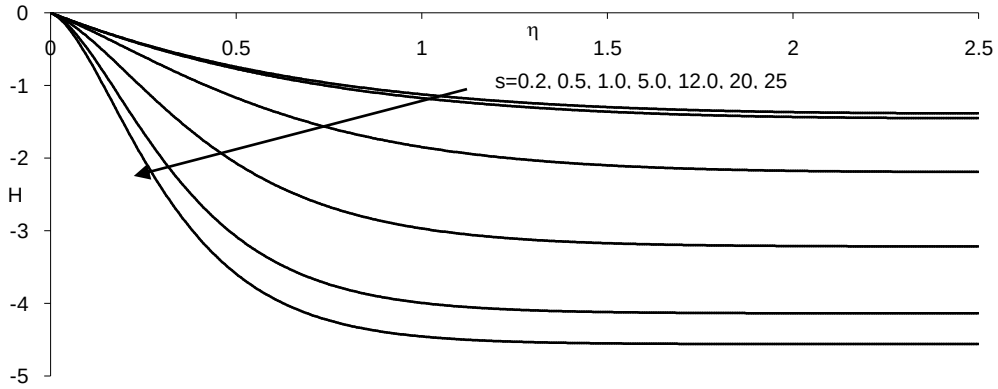

Fig.4: Graph of *H* for different values of the parameter *s*

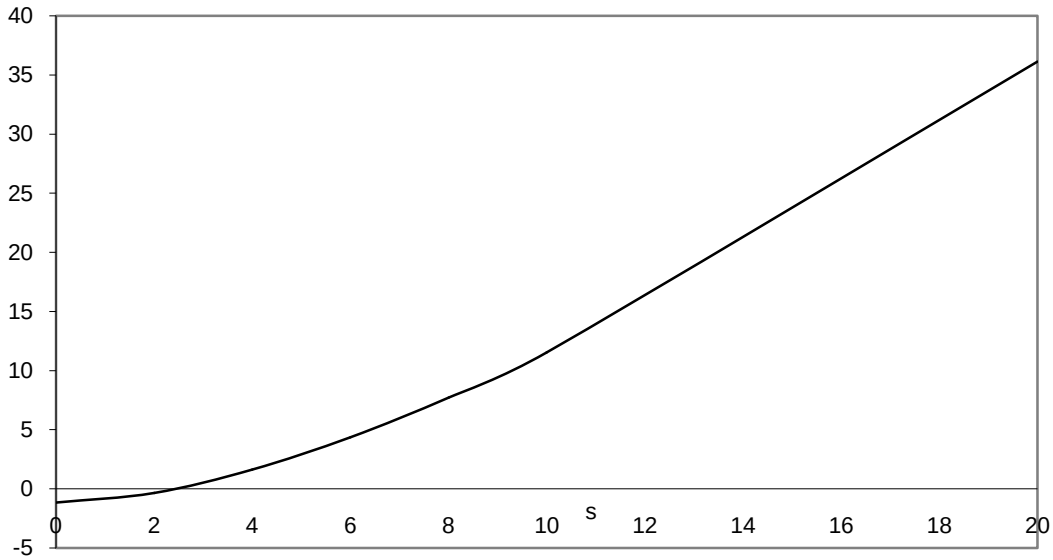

Fig .5: Graph of $F'(0)$ for different small values of the parameter s

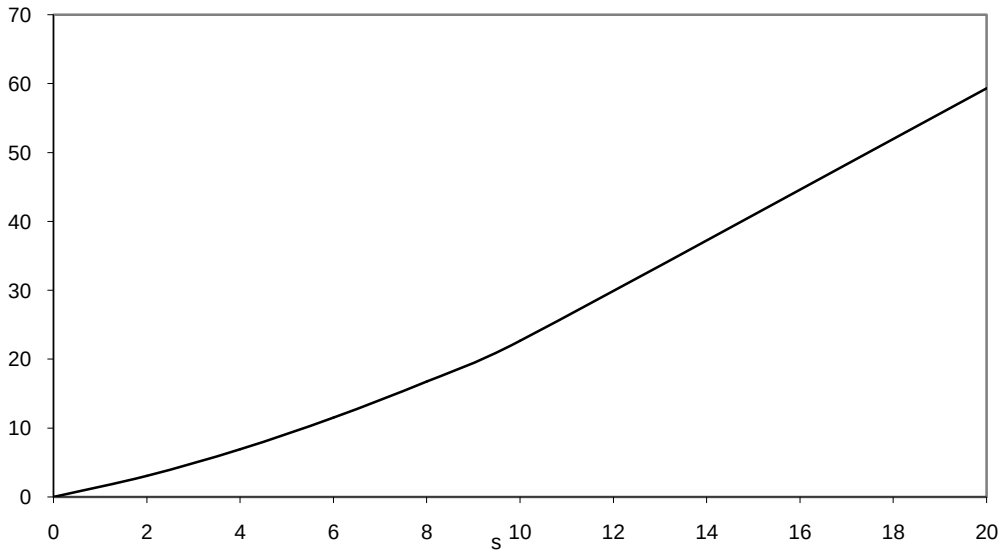

Fig .6: Graph of $-G'(0)$ for different small values of the parameter s

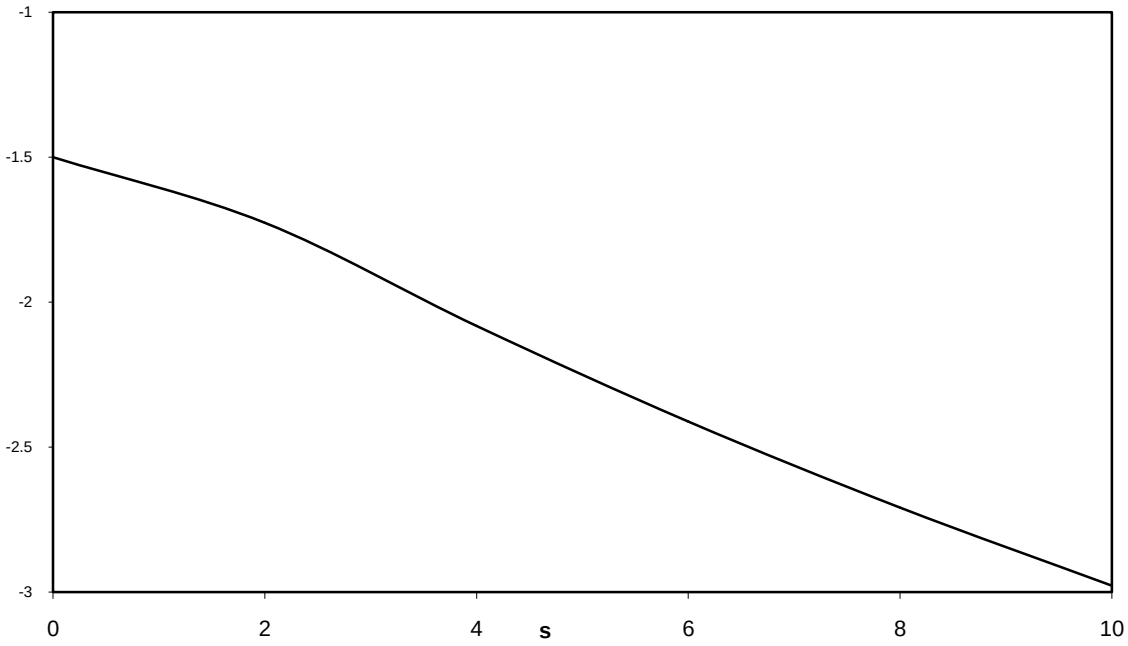

Fig .7: Graph of $H(\infty)$ for different small values of the parameter s

Fig.8: Graph of $P(\infty)$ for different small values of the parameter s

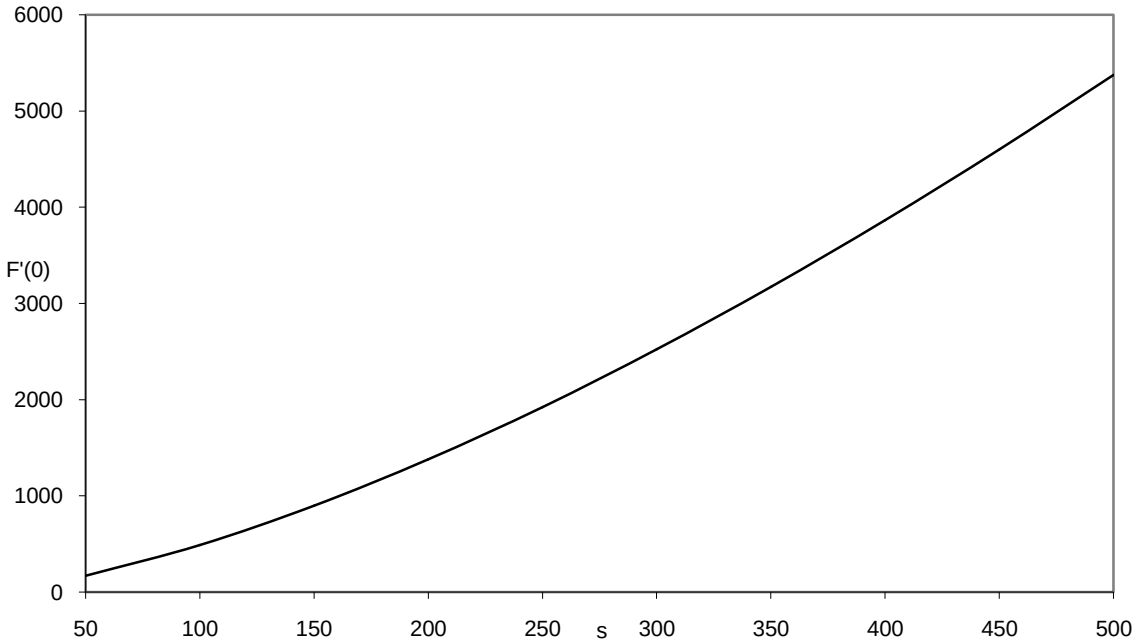

Fig .9: Graph of $F'(0)$ for different large values of the parameter *s*

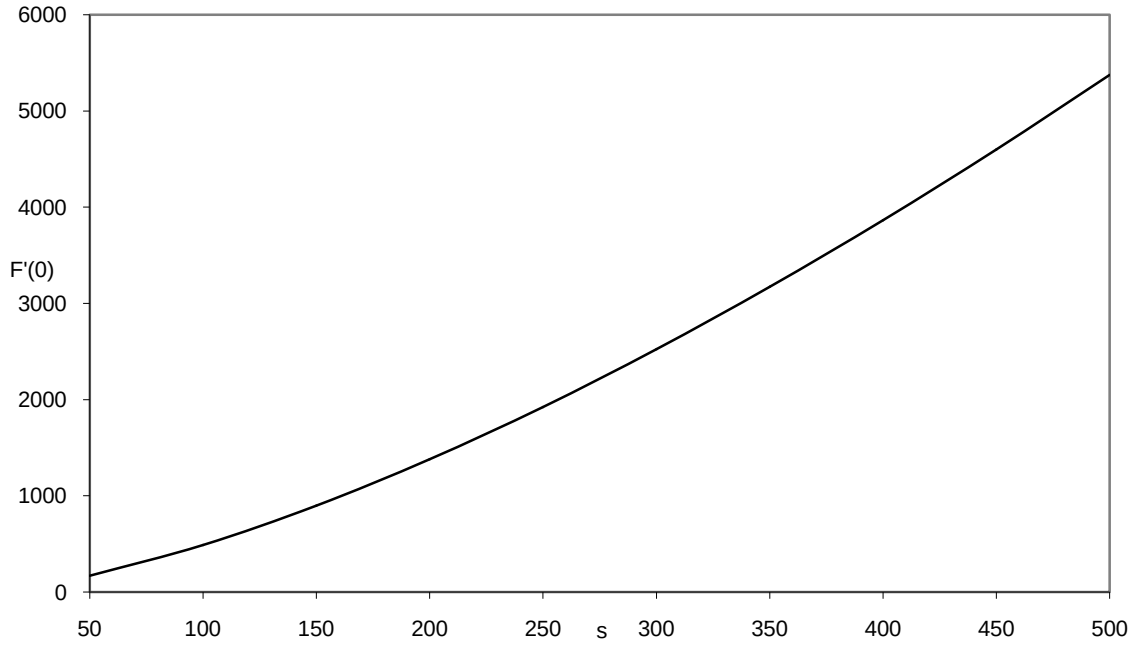

Fig .10: Graph of $-G'(0)$ for different large values of the parameter *s*

REFERENCES

[1] Sakiadas, B. C. (1961). Boundary layer behavior on continuous solid surface: I. Boundary -layer equations for two-dimensional and axisymmetric flow, J. AlChe, 7:221-225.

[2] Sakiadas, B. C. (1961). Boundary layer behavior on continuous solid surface: I.I Boundary- layer equations for two-

dimensional and axisymmetric flow, J. AlChe, 7: 26-28.

[3] Crane, L. J. (1970). Flow past a stretching plate Zeit. Angew. Math. Phys. 21:645-647.

[4] Wang, C. Y. (1984). The three-dimensional flow due to a stretching flat surface, Phys. Fluids 27:1915.

[5] Chiam, T. C. (1994). Stagnation-Point flow towards a stretching plate, J. Phys. Soc. Japan 63:2443-2444.

[6] Mahaputra, T. R. & Gupta, A. S. (2004). Heat transfer in stagnation-point flow towards a stretching surface, Heat Mass Transfer, 38: 811-820.

[7] Mahaputra T. R. & Gupta, A. S. (2003). Stagnation-point flow towards a stretching surface, Can. J. Chem.Eng.81 258-263.

[8] Carrgher, P. & Crane, L.J. (1982). Heat transfer on a continuous stretching sheet, J. Appl. Math. Mech (ZAMM), 62:564-565.

[9] Gupta, P.S. & Gupta, A.S. (1982). Heat and mass transfer on a stretching sheet with suction or blowing, Can. J. Appl. Math. Mech (ZAMM), 62: 564-565.

[10] Liao, S.J. & Pop, I. (2004). On explicit analytic solutions of boundary layer equations about flows in a porous medium or for stretching walls. Int.J. Heat Mass Transfer, 47:75-85.

[11] Shafique, M. & Rashid, A. (2005). The numerical methods for the 3-dimensional flow due to a stretching flat surface Int. J. of Applied Math. 17(1): 15-26.

[12] Hussain, S. & Kamal, M.A. (2013). Flow of micropolar fluid over a stretchable disk, World Applied Sciences Journal 25 (4): 600-606.

[13] Von Karaman, T. (1921). Uber laminare und turbulent Reibung Z. Agnew Math.Mech.1: 233-252.

[14] Rosehead, L. (1963). Laminar Boundary Layer, Oxford University Press, Oxford.

[15] Schlichting, H. (1991). Boundary Layer Theory, 6th edition, McGraw-Hill, New York.

[16] Kohama, Y. (1984). Study on boundary layer transition of a rotating disk, Acta Mech.50:193-199.

[17] Watanabe, T. (1985). Stability of boundary layers along a rotating disk, Trans. Japan Soc. Mech. Eng, 51:3344-3347.

[18] Hussain, S. Ahmad, F., Shafique, M. & Hussain S. (2013). Numerical solution for deceleration of a rotating disk, International Journal of Emerging Technology and Advanced Engineering, Vol. 3 (5):718-725.

[19] Fang, T. (2007). Flow over a stretchable disk, Phys. Fluids 19, 128105:1-4.

[20] Smith, G.D. (1979). Numerical Solution of Partial Differential Equation, Clarendon Press, Oxford.

[21] Gerald, C. F. (1989). Applied Numerical Analysis, Addison-Wesley Pub. NY.

[22] Milne, W. E. (1970). Numerical Solution of Differential Equation, Dover Pub.

[23] Burden, R. L. (1985). Numerical Analysis, Prindle, Weber & Schmidt, Boston.